ELSEVIER

PII: S0032-3861(97)00486-2

Polymer Vol. 39 No. 10, pp. 1999–2009, 1998

0032-3861/98/$19.00+0.00

Binary interaction parameters from blends of SMA copolymers with TMPC–PC copolycarbonates

G. D. Merfeld and D. R. Paul*
Department of Chemical Engineering and Center for Polymer Research, University of Texas at Austin, Austin, TX 78712, USA
(Received 11 March 1997; revised 2 June 1997)

Miscibility maps for blends of copolycarbonates based on various proportions of tetramethyl bisphenol-A and bisphenol-A (TMPC–PC) with copolymers of styrene–maleic anhydride (SMA) have been established and interaction energies have been calculated from the data using a binary interaction model combined with the Flory–Huggins theory. This analysis provides an independent assessment of all six interaction energies between the various repeat unit pairs. These include the first reported estimates for the binary interaction energies of MA with TMPC and with PC. The other four interaction energy values found here are in excellent agreement with earlier reports. LCST-type phase separation temperatures were determined and compared with values predicted by the Sanchez–Lacombe equation-of-state theory. © 1998 Elsevier Science Ltd. All rights reserved.

(Keywords: blends; polycarbonates; styrene/maleic anhydride copolymer)

INTRODUCTION

Commercial blends of polycarbonate (PC) with acrylonitrile–butadiene–styrene (ABS) materials generally have adequate properties without the use of a compatibilizer owing to the nature of the thermodynamic interactions between PC and the styrene–acrylonitrile (SAN) matrix of ABS. Extensive research has accurately quantified the PC/SAN interaction, and the results may be used to optimize blend performance[1–11]. There has been recent interest in blends of PC with styrene–maleic anhydride (SMA) copolymers[12]. To rationally evaluate the opportunities afforded by such blends, it is useful to determine the PC/SMA interaction. Blends of PC with SMA copolymers are completely immiscible; however, prior work has shown that tetramethyl polycarbonate (TMPC) is miscible with SMA copolymers containing limited amounts of MA[13]. With this knowledge, a strategy to probe polymer interactions can be devised through the use of copolymers to dilute the unfavourable PC/SMA interactions employing the repeat-unit-based accounting procedures of a binary interaction model[14–16]. This will create an envelope of miscibility in the isothermal phase map of SMA copolymer composition *versus* TMPC–PC copolycarbonate composition. The boundary separating miscible and immiscible blend compositions can then be used to extract interaction energy estimates, thus allowing the verification or refinement of previously determined interaction energies and the evaluation of unknown interaction energies. Furthermore, once binary interaction energies for the blend system are known, equation-of-state theory can be used to predict phase separation behaviour for comparison with experimental observations.

* To whom correspondence should be addressed

POLYMER BLEND THERMODYNAMICS

The Gibbs free energy of mixing per unit volume for a binary system of monodisperse polymers can be modelled by the Flory–Huggins theory[17,18]

$$\Delta g_{mix} = RT\left(\frac{\rho_A\phi_A \ln \phi_A}{M_A} + \frac{\rho_B\phi_B \ln \phi_B}{M_B}\right) + B\phi_A\phi_B \quad (1)$$

where R is the gas constant, T is the absolute temperature, and ρ_i, ϕ_i, and M_i are the density, volume fraction and molecular weight of component i, respectively. The interaction energy density B includes the heat of mixing plus other non-combinatorial effects. An expression for the spinodal condition can be derived from equation (1) if it is assumed that B is not a function of composition

$$\frac{d^2\Delta g_{mix}}{d\phi_1^2} = RT\left(\frac{\rho_A}{\phi_A M_A} + \frac{\rho_B}{\phi_B M_B}\right) - 2B_{sc} = 0 \quad (2)$$

However, if B is dependent on composition, a new interaction energy at the spinodal condition, denoted B_{sc}, is defined by equation (2). At the critical conditions of temperature and blend composition, where the third derivative of Δg_{mix} with respect to composition is exactly zero and the system lies on the boundary between miscible and immiscible, the balance between the combinatorial entropy and component interactions is described by

$$B_{crit} = \frac{RT}{2}\left[\sqrt{\frac{\rho_A}{(\bar{M}_W)_A}} + \sqrt{\frac{\rho_B}{(\bar{M}_W)_B}}\right]^2 \quad (3)$$

where $(\bar{M}_W)_i$ is the weight-average molecular weight[19–22]. At a given temperature, miscibility is predicted when the net interaction energy for a blend is more favourable than B_{crit}.

For a blend of two homopolymers, B is simply the interaction energy between the two repeat units involved. However, for blends of homopolymers with copolymers or for blends of two copolymers, a model must be invoked to

account for the multiple intramolecular and intermolecular interactions that contribute to the net interaction energy density B in equation (1). The binary interaction model accounts for such interactions and has been used with considerable success for interpreting the phase behaviour of blends involving copolymers[14–16]. It has the following form for a blend of two copolymers

$$B = B_{13}\phi_1'\phi_3'' + B_{14}\phi_1'\phi_4'' + B_{23}\phi_2'\phi_3'' + B_{24}\phi_2'\phi_4'' - B_{12}\phi_1'\phi_2' - B_{34}\phi_3''\phi_4'' \quad (4)$$

where repeat units 1 and 2 are randomly incorporated with volume fractions ϕ_1' and ϕ_2' in the first copolymer, and repeat units 3 and 4 are likewise incorporated in the second copolymer with volume fractions ϕ_3'' and ϕ_4''. The binary interaction model simplifies to the following expression

$$B = B_{12}(\phi_2'')^2 \quad (5)$$

for a homopolymer/copolymer blend where repeat units of type 1 are common to both polymers and where ϕ_2'' is the volume fraction of type 2 repeat units in the copolymer. Clearly, when the homopolymer and copolymer share a common repeat unit, there is only one binary interaction and it may be determined independently of previously evaluated interaction energies.

The Flory–Huggins theory as presented here can predict only UCST-type phase boundaries unless an empirical temperature dependence is introduced into the interaction energy B. However, most polymer blends, including those investigated in this study, show LCST-type phase behaviour. Equation-of-state theories account for the compressible nature of polymer mixtures and can predict LCST-type phase separation. The lattice-fluid theory of Sanchez and Lacombe[23–29] is used in this work; however, only a brief overview is given here. More detailed discussion and a review of its application to polymer blends can be found elsewhere[30,31]. The Sanchez–Lacombe equation of state is given by

$$\tilde{\rho}^2 + \tilde{P} + \tilde{T}\left[\ln(1-\tilde{\rho}) + \left(1 - \frac{1}{r}\right)\tilde{\rho}\right] = 0 \quad (6)$$

in terms of the reduced variables $\tilde{P} = P/P^*$, $\tilde{T} = T/T^*$, $\tilde{\rho} = \rho/\rho^* = v^*/v$, where P and v are pressure and specific volume, respectively, and r is the chain length defined as

$$r = \frac{MP^*}{kT^*\rho^*} = \frac{M}{v^*\rho^*} \quad (7)$$

Variables with asterisks denote equation-of-state characteristic parameters with mixing rules as given by Sanchez and Lacombe[25]. The spinodal condition has been derived as

$$\frac{d^2G}{d\phi_1^2} = \frac{1}{2}\left(\frac{1}{r_1\phi_1} + \frac{1}{r_2\phi_2}\right) - \tilde{\rho}\left(\frac{\Delta P^* v^*}{kT} + \frac{1}{2}\psi^2\tilde{T}P^*\beta\right) = 0 \quad (8)$$

where ψ is a dimensionless function reviewed elsewhere[25] and β is the isothermal compressibility. In the Sanchez–Lacombe theory, the bare interaction energy density, ΔP^*, is analogous to B of the Flory–Huggins theory stripped of equation-of-state effects. The binary interaction model shown in equation (4) for B may also be expressed in terms of ΔP^* as

$$\Delta P^* = \Delta P^*_{13}\phi_1'\phi_3'' + \Delta P^*_{14}\phi_1'\phi_4'' + \Delta P^*_{23}\phi_2'\phi_3'' + \Delta P^*_{24}\phi_2'\phi_4'' - \Delta P^*_{12}\phi_1'\phi_2' - \Delta P^*_{34}\phi_3''\phi_4'' \quad (9)$$

where volume fractions are based on hard core volumes. Furthermore, if the volume fractions used in the Flory–Huggins theory are assumed to be equivalent to those used in the Sanchez–Lacombe theory, the Flory–Huggins interaction energy and the bare interaction energy can be related[30,32]

$$B_{sc} = \tilde{\rho}\Delta P^* + \left\{[P_2^* - P_1^* + (\phi_2 - \phi_1)\Delta P^*] + \frac{RT}{\tilde{\rho}}\left(\frac{1}{r_1^0 v_1^*} - \frac{1}{r_2^0 v_2^*}\right) - RT\left[\frac{\ln(1-\tilde{\rho})}{\tilde{\rho}^2} + \frac{1}{\tilde{\rho}}\right] \times \left(\frac{1}{v_1^*} - \frac{1}{v_2^*}\right)\right\}^2 \times \left\{\frac{2RT}{v^*}\left[\frac{2\ln(1-\tilde{\rho})}{\tilde{\rho}^3} + \frac{1}{\tilde{\rho}^2(1-\tilde{\rho})} + \frac{(1-1/r)}{\tilde{\rho}^2}\right]\right\}^{-1} \quad (10)$$

where r_i^0 is the number of sites occupied by molecule i in the pure close-packed state such that $r_i^0 v_i^* = r_i v^*$.

MATERIALS AND PROCEDURES

The polymers used in this study are listed in *Table 1* and *Table 2* along with their physical properties. The polystyrene (PS), Cosden 550, was obtained from Cosden Oil and Chemical Co., while the SMA copolymers were obtained from Arco Chemical Co. and Dow Chemical Co. as indicated. The numerical suffix on the copolymer acronym indicates the weight per cent of MA. Three of the SMA copolymers, SMA9, SMA10.7 and SMA12.2, contain rubber particles added by the manufacturer to improve impact resistance. The PC is Lexan 131-111 from General Electric Co. and the TMPC is from Bayer AG. TMPC–PC copolycarbonates were synthesized in our laboratory using an interfacial polymerization technique described previously[4,33]. The suffix on the copolycarbonate code indicates the weight per cent of TMPC. Molecular weight information was determined by gel permeation chromatography calibrated with polystyrene standards.

Polymer blends of 50/50 composition by weight of TMPC–PC and SMA copolymers were cast from a common solvent, either dichloromethane, DCM, or tetrahydrofuran, THF. Blends containing SMA copolymers with rubber modifier were prepared on a rubber-free basis by subtracting the weight of the rubber from the actual SMA weight; thereby, the correct SMA to TMPC–PC blend ratio was maintained. Films from DCM solutions were cast at room temperature by evaporation from an open beaker, allowed to dry overnight, and then annealed for up to 96 h in a vacuum oven at 180°C. At room temperature, DCM solutions containing 2 wt.% of polymer dried into films within 2 h. Blends were also hot cast from DCM and THF by pouring 2 wt.% polymer solutions on to a glass plate maintained at 50°C and 60°C, respectively. The films were dry to the touch within 3 min but were allowed to remain on the glass plate for an additional 5 min before they were removed and annealed in a vacuum oven at 180°C for up to 96 h.

Glass transition temperatures were determined and blend miscibility was assessed with a Perkin-Elmer DSC-7 system using a scan rate of 20°C min^{-1}. Two scans were performed: the first to erase the thermal history and the second to evaluate the thermal characteristics. Both the onset and the

Table 1 Styrene polymers used in this study

Polymer	MA	Molecular weight information[a]		T_g (°C)		Source
	(wt.%)	$\bar{M}_n$	$\bar{M}_w$	Onset	Endpoint	
Polystyrene (PS)						
PS(330)	0	100000	330000	98	103	Cosden Oil and Chemical Co. (Cosden 550)
PS(52)	0	50500[b]	52000[b]	103	–	Polymer Laboratories Ltd.
PS(35)	0	34200[b]	35000[b]	102	–	Polymer Laboratories Ltd.
PS(22)	0	21000[b]	22000[b]	102	–	Polymer Laboratories Ltd.
PS(17)	0	16300[b]	17500[b]	101	–	Polymer Laboratories Ltd.
PS(9.2)	0	8900[b]	9200[b]	96	–	Polymer Laboratories Ltd.
Poly(styrene–co–maleic anhydride)						
SMA2	2	183000	320000	105	112	Arco Chemical Co.
SMA4.7	4.7	94000	179000	106	115	Dow Chemical Co.
SMA6	6	152000	273000	110	118	Arco Chemical Co.
SMA8	8	100000	200000	115	123	Arco Chemical Co.
SMA9[c]	9	100000	240000	115	124	Arco Chemical Co.
SMA10.7[d]	10.7	100000	210000	118	127	Arco Chemical Co.
SMA12.2[c]	12.2	91000	190000	119	130	Arco Chemical Co.
SMA13	13	108000	203000	127	136	Arco Chemical Co.
SMA14	14	92000	178000	125	133	Arco Chemical Co.
SMA17	17	52000	114000	132	141	Arco Chemical Co.
SMA18.1	18.1	92000	260000	135	143	Dow Chemical Co.

[a]Determined by g.p.c. analysis using PS standards
[b]Provided by supplier
[c]Contains 16% rubber by weight
[d]Contains 5% rubber by weight

Table 2 Polycarbonates used in this study

Polymer	PC	Molecular weight information[a]		T_g (°C)		Source
	(wt.%)	$\bar{M}_n$	$\bar{M}_w$	Onset	Endpoint	
TMPC	0	13700	37900	190	199	Bayer AG
TMPC95	5	10800	32700	181	191	Synthesized[b]
TMPC90	10	8600	49400	172	184	Synthesized[c]
TMPC85	15	7300	29900	175	185	Synthesized[c]
TMPC83	17.5	8700	39500	183	191	Synthesized[b]
TMPC80	20	8800	31300	177	185	Synthesized[b]
TMPC75	25	7500	34300	174	187	Synthesized[c]
PC	100	37000	76500	147	158	General Electric Co. (Lexan 131-111)

[a]Determined by g.p.c. analysis using PS standards
[b]Ref. [33]
[c]Ref. [4]

endpoint of the glass transitions were recorded; the onset T_g was evaluated at the intersection of the pre-event baseline and a line drawn tangentially to the inflection point, while the endpoint was evaluated at the intersection of the inflection point tangent and the baseline established after the thermal event.

In the evaluation of polymer blend miscibility, the number of T_gs, their location, and their breadth were considered. Blends with a single, narrow T_g were judged miscible, while blends with two distinct or slightly overlapping T_gs were evaluated as immiscible. The non-equilibrium blend phase behaviour was investigated when the differential thermal calorimetry (d.s.c.) scans showed a single but broad T_g, or when it showed significantly shifted T_gs. Phase separation temperatures were evaluated by d.s.c. using a temperature programme of annealing followed by a scan to assess the miscibility. Annealing for times of 5–60 min was performed in the differential scanning calorimeter while for longer times, up to several days, annealing was performed in a vacuum oven. A series of experiments was performed to bracket the phase separation temperature; at temperatures below this value, annealing failed to induce a change in miscibility, while annealing at temperatures above this value led to two T_gs. When possible, the reversibility of the phase behaviour was investigated by annealing a two-phase blend at a temperature below its observed phase separation temperature but well above the blend T_g. A change from two T_gs to a single T_g confirmed that an equilibrium phase boundary was crossed.

When possible, visual assessment of the phase behaviour was used to confirm the d.s.c. evaluations. Refractive indices were estimated by group contribution methods, and for all blend pairs the difference was estimated to be greater

Table 3 Summary of published interaction energies

Interaction pair	ΔP_{ij}^* (cal cm^{-3})	B_{ij} (cal cm^{-3})	Evaluation temp. (°C)	$B_{ij}{}^a$ (cal cm^{-3})	System	Reference
TMPC/PC	− 0.25	− 0.32	140	− 0.10	TMPC–PC/SAN	4
TMPC/PC	− 0.23	− 0.33	140	− 0.08	TMPC–PC/SMMA	4
TMPC/PS	− 0.17	0.02	240	− 0.09 to − 0.02	TMPC/PS	32
TMPC/MA	10.6[b]	10.0[b]	170	9.7 to 10.2	TMPC/SMA	13
PC/PS	0.44	0.43	50	0.40 to 0.41	PC/PS	35
PC/PS	0.49	–	–	0.44 to 0.45	PC/SMMA	35
PC/PS	0.43	0.49	140	0.39 to 0.40	TMPC–PC/SAN	4
PC/PS	0.41	0.61	140	0.37 to 0.39	TMPC–PC/SMMA	4
PS/MA	11.5[c]	10.7	170	10.4 to 10.7	PMMA/SMA	13

[a]Calculated at 180°C
[b]Recalculated using reported miscibility boundaries and temperature corrected B_{ij}
[c]Conversion of B_{ij} to ΔP_{ij}^* recalculated using the characteristic parameters reported in Table 4

Table 4 Sanchez–Lacombe characteristic parameters

Repeat unit type	Parameter code	P^* (MPa)	T^* (K)	ρ^* (g cm^{-3})	Temperature range (°C)	Reference(s)
TMPC	TMPC	440	729	1.185	220–270	32
PC	PC	496	802	1.276	220–280	39
PS[a]	PS180	385	781	1.101	180–230	13, 31
PS[a]	PS200	379	795	1.097	200–250	13, 31
PS	PS220	373	810	1.092	220–270	32
MA[a,b]	MA180	656	832	1.540	180–230	13, 31
MA[a,b]	MA200	477	915	1.551	200–250	13, 31
MA[b]	MA220	423	946	1.578	220–270	13, 31

[a]Recalculated from data in reference
[b]Based on an extrapolation of SMA copolymer characteristic parameters

than 0.05; as a general rule, a refractive index difference of 0.01 is sufficient to use visual evaluation to determine the miscibility[34]. The use of visual evaluation was limited, however, to blends where the polymers were transparent prior to blending. For this reason, SMA copolymers containing rubber could not be evaluated optically. Additionally, several of the TMPC–PC copolymers appeared to have particulate contamination that precluded any visual assessment. The filtration of solutions of blends containing these TMPC–PC copolymers or rubber-modified SMA did not improve the optical clarity but had no effect on the miscibility behaviour observed by d.s.c.

SUMMARY OF PREVIOUSLY EVALUATED INTERACTION ENERGIES

To completely describe the phase behaviour for blends of TMPC–PC copolycarbonates with SMA copolymers, six binary interaction energies are required, as may be seen in equation (4) or alternatively in equation (9). These interactions correspond to those that occur between each of the four repeat units involved. All but two of the interactions relevant to the current blend system have been previously quantified with considerable confidence and verified in many cases by several methods or by independent studies. *Table 3* is a summary of the most refined estimates of these interaction energies available to date and a discussion of their evaluation follows.

Kim and Paul investigated the TMPC/PC interaction in two independent studies by blending TMPC–PC copolymers with SAN copolymers and with SMMA copolymers[4]. Binary interaction energies were evaluated from isothermal miscibility data by fitting the Flory–Huggins theory combined with the binary interaction model to the boundary between miscible and immiscible blends. The reported values of − 0.32 and − 0.33 cal cm^{-3} for $B_{\text{TMPC/PC}}$ are in excellent agreement. In the same study, estimates for $B_{\text{PC/PS}}$ of 0.49 and 0.61 were made. The PC/PS interaction was further probed by Callaghan and Paul using the critical molecular weight technique[35]. The phase separation behaviour of PC blends with PS of varying molecular weights was modelled by both the Flory–Huggins theory and the Sanchez–Lacombe equation-of-state to obtain interaction energies of $B_{\text{PC/PS}} = 0.43$ and $\Delta P^*_{\text{PC/PS}} = 0.44$. These values are in good agreement with those determined by Kim. A thorough investigation of the TMPC/PS interaction was reported by Kim and Paul using homopolymer blends and an equation-of-state analysis of phase separation behaviour[32]. The reported bare interaction of $\Delta P^*_{\text{TMPC/PS}} = -0.17$ cal cm^{-3} is in line with studies made on the system using light and neutron scattering[36–38]. By investigating blends of SMA copolymers with SMMA copolymers and with SAN copolymers, Gan and Paul offered a refined estimate of $B_{\text{PS/MA}} = 10.7$[13]. Additionally, an approximate range for $B_{\text{TMPC/MA}}$ of 11.3–11.7 cal cm^{-3} was reported using the miscibility limit for SMA copolymers with TMPC. The latter values contain an error in accounting for the temperature dependence of the binary interactions, which when properly corrected changes the approximated $B_{\text{TMPC/MA}}$ range to 9.9–10.1 cal cm^{-3}.

For each Flory–Huggins interaction energy in *Table 3*, an evaluation temperature is reported. Equation (10) was used to correct B_{ij} values to 180°C, and thereby allow comparison with the B_{ij} interactions determined in this study. For these calculations, bare interaction energies (ΔP^*_{ij}) were assumed to be independent of temperature, an assumption that is reasonable in the absence of strong specific interactions and that is tantamount to saying that interactions do not depend on spatial orientation but only the distance between molecules. Equation-of-state theory accounts for the latter by considering changes in density with temperature. The characteristic parameters in the Sanchez–Lacombe equation of state, used for the temperature corrections of B_{ij}, are listed in *Table 4* for each of the repeat unit types. It should be noted that the characteristic parameters for MA are based on an extrapolation of the parameters for SMA copolymers to 100% MA since the homopolymer cannot be synthesized, and therefore, cannot be characterized directly[13]. Three sets of parameters are reported for both PS and MA corresponding to temperature ranges of 180–230°C, 200–250°C, and 220–270°C. The effect of using these different parameter sets is reflected in the ranges reported for B_{ij} at 180°C. Overall, the calculated variation is small compared to the magnitude of the interaction energy itself. The effect of characteristic parameter sets on equation-of-state-based analyses will be considered further in a later section.

EVALUATION OF S/MA INTERACTION ENERGY

At least one B_{ij} value must be known from an independent study to extract binary interactions from the copolymer/copolymer isothermal miscibility map investigated in this study. Any of the previously determined B_{ij} values summarized in *Table 3* could be used for this purpose. Moreover, all the well-established interaction values could be held fixed in the binary interaction model to reduce the number of unknowns. This approach may increase the accuracy of newly evaluated parameters, but on the other hand, errors included in previously evaluated B_{ij} could, potentially, offset the benefits of this strategy. A model study would independently evaluate all interactions, confirming or refining earlier estimates while determining unknown values. For these reasons, an independent evaluation of $B_{PS/MA}$ was investigated.

By blending a homopolymer and a copolymer that share a common repeat unit, the reduced form of the binary interaction model shown in equation (5) makes it possible to independently evaluate the associated binary interaction. For example, PS and SMA blends are miscible when the MA content is low but become immiscible as the MA content is increased[13]. The binary interaction energy $B_{PS/MA}$ can be estimated when the copolymer compositions that define the miscibility boundary are known. The critical molecular weight technique is an alternative approach that is applicable when the interaction energy lies in a range such that changes in molecular weight can induce a change in the phase behaviour[40,41]. Repeat unit interactions are held constant (*i.e.* the blend ratio and copolymer composition are fixed) while the entropic contribution to the free energy of mixing is raised or lowered by changing either of the polymer molecular weights.

A more refined estimate for the S/MA interaction can be evaluated by combining both techniques to investigate the miscibility boundary created by concurrently changing the copolymer composition and homopolymer molecular weight. For this study, the polystyrenes listed in *Table 1* were blended with SMA copolymers. *Figure 1* shows the blends found to be miscible or immiscible, denoted as empty or filled symbols, respectively, on a plot of weight per cent of MA in SMA *versus* PS weight-average molecular weight. Blends represented by empty circles were prepared by solvent casting and annealing at 170°C, while the filled circles represent blends prepared by melt mixing at 170°C. The phase behaviour of blends prepared by both techniques is in agreement except near the miscibility boundary, where blends represented by the empty squares were found to be homogeneous when melt-mixed but were phase separated when solvent-cast. Because melt-mixed blends are not susceptible to solvent-induced effects, the results for these blends were used for evaluation of the interaction energy.

By equating equation (3) and (5), an expression for the border between miscible and immiscible blends of PS with SMA copolymers can be derived

$$\phi_{MA} = \sqrt{\frac{RT}{2B_{PS/MA}}}\left[\sqrt{\frac{\rho_{SMA}}{(\bar{M}_W)_{SMA}}} + \sqrt{\frac{\rho_{PS}}{(\bar{M}_W)_{PS}}}\right] \quad (11)$$

This result assumes that the 50/50 blend compositions used in the experiments match or deviate only slightly from the actual critical compositions. The severity of this assumption is investigated later in this paper. If, to a good approximation, the first term within the square brackets in equation (11), can be represented by a constant, then the slope from a plot of ϕ_{MA} *versus* $\sqrt{\rho_{PS}/(\bar{M}_W)_{PS}}$ will allow the evaluation of $B_{PS/MA}$. Such a plot is shown in *Figure 2*. The line separating miscible from immiscible blends was fitted to the data by a linear regression forced to pass through a *y*-intercept consistent with the calculated average $\sqrt{\rho_{SMA}/(\bar{M}_W)_{SMA}}$. An estimate of $B_{PS/MA} = 10.6$ cal cm^{-3} was obtained by this analysis, which is in good agreement with the estimate obtained by Gan and Paul[13]. The phase boundary shown in *Figure 1* was calculated from this value of $B_{PS/MA}$ using equation (11).

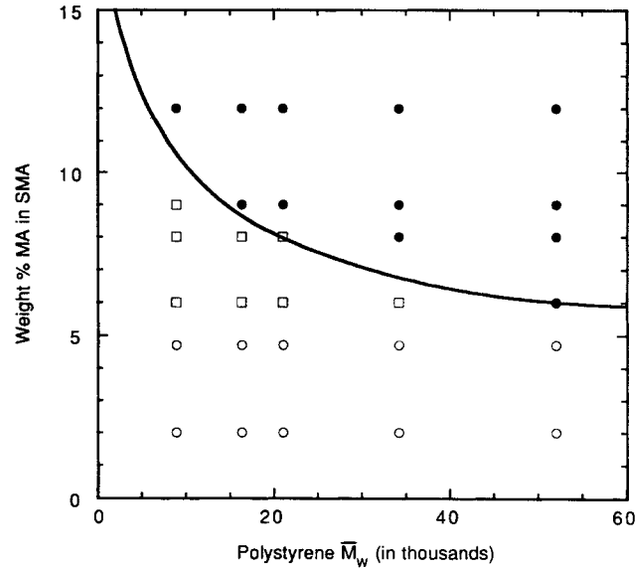

Figure 1 Miscibility behaviour for 50/50 blends of SMA copolymers with monodisperse polystyrenes of varying molecular weight. (○) Judged miscible as prepared by solvent casting; (□) judged miscible as prepared by melt mixing; (●) immiscible. The curve fit to the boundary between miscible and immiscible blends is based on $B_{PS/MA} = 10.6$ cal cm^{-3}

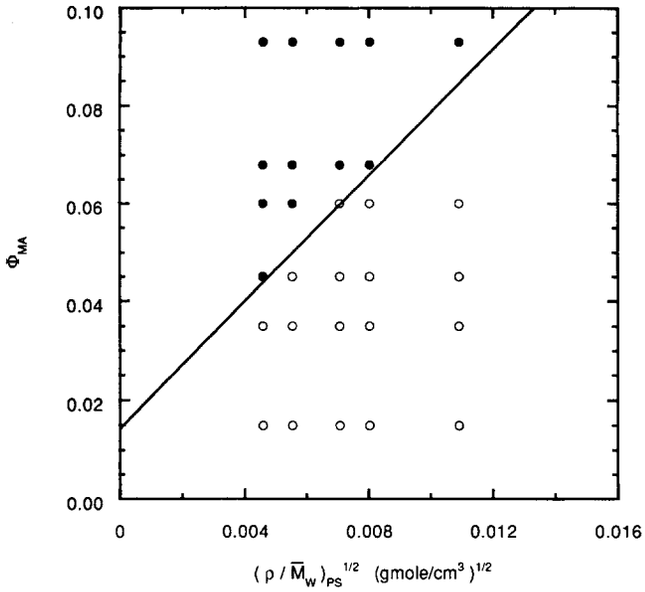

Figure 2 Graphical analysis of equation (11) to evaluate the $B_{PS/MA}$ interaction energy from the slope of the line separating (○) miscible from (●) immiscible blends of SMA coploymers with PS of varying molecular weights

ISOTHERMAL MISCIBILITY MAP

The d.s.c. evaluation of the miscibility of various TMPC–PC/SMA pairs at 180°C was aided by graphical constructions that allow simultaneous comparison of the measured *versus* the predicted (assuming miscibility) glass transitions for blends of copolymers. In these graphs, an example of which is shown in *Figure 3* for blends of TMPC80 with a range of SMA copolymers, the shaded zones are established between the onset and endpoint glass transitions for the unblended copolymers. A third zone is then predicted for a miscible blend using the Fox equation[42]

$$\frac{1}{T_g} = \frac{w_1}{T_{g1}} + \frac{w_2}{T_{g2}} \tag{12}$$

where w_i and T_{gi} are component i mass fractions and glass transitions, respectively. By overlaying measured blend transition temperatures on the three shaded zones, interpretation of the d.s.c. results is simplified, and for the example shown, a window of miscibility is easily identified for blends with SMA copolymers containing between 6 and 10 wt.% MA. Furthermore, this analysis may help to identify partial miscibility evidenced by broadened or shifted T_gs.

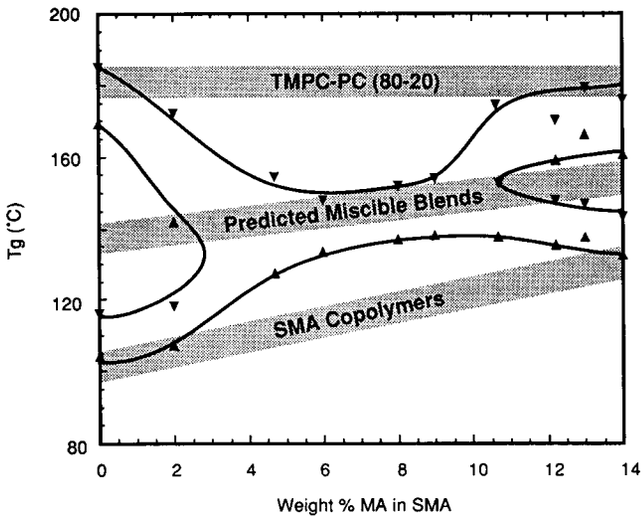

Figure 3 Example of graphical analysis used to evaluate the blend miscibility. Measured (▲) onset and (▼) endpoint of the glass transition region for blends of TMPC80 with SMA copolymers overlaid on shaded glass transition zones measured for the pure copolymers and predicted for their miscible blends via the Fox equation

Establishing that a blend has either one or two phases does not guarantee that the equilibrium state of miscibility or immiscibility is known, since blend preparation techniques can sometimes produce non-equilibrium phase behaviour. For instance, the so-called 'solvent' effect can lead to a phase separated mixture when a miscible pair is cast from a common solvent[43–46]. This effect is caused by an asymmetry in the polymer–solvent interactions which gives rise to a closed region of immiscibility in the ternary solvent–polymer–polymer phase diagram[44]. A blend may become trapped within this region during casting, leading to heterogeneity of the resulting blend when the two polymers are indeed miscible. Solvent casting can also produce homogenous blends that are actually immiscible, as was demonstrated for blends of PC with poly(methyl methacrylate)[47,48]. When the polymer solution becomes concentrated during casting, the mixture cannot reach its equilibrium state because of limited molecular mobility. Rapid solvent removal can exacerbate the latter mobility effect but can help avoid the previously mentioned solvent effect. In either case, when phase separation or phase dissolution kinetics are slow, very long annealing times may be required for blends to reach their equilibrium state. Therefore, special consideration must be exercised when using a solvent-based preparation method, including the appropriate choice of solvent, casting technique and annealing programme.

The complete matrix of TMPC–PC and SMA copolymer blends were prepared by solvent casting from DCM. The samples were annealed at 180°C for 48 h under vacuum, evaluated for miscibility, returned to the vacuum oven for an additional 48 h, and then re-evaluated for miscibility. The additional annealing altered the phase behaviour of several blends along the miscibility border, causing them to change from two-phase to one-phase, thus expanding the envelope of observed miscibility. Blends prepared by hot casting from DCM showed the same phase behaviour. These observations suggest that solvent effects during DCM casting may have left blends trapped in a non-equilibrium state. For slow kinetics of phase separation, longer annealing times may allow the system to reach equilibrium, and blends determined to have two phases after short annealing times could become homogeneous mixtures with longer annealing times — as was observed. In general, the miscibility region opened to higher MA contents with increased annealing time, but this was only evident when the copolycarbonate contained 10 wt.% or more PC and the SMA copolymer contained 6 wt.% or more MA. The copolymer composition has a dramatic effect on the glass transition temperature, as shown in *Table 1* and *Table 2*, and can significantly affect molecular mobility. Maleic anhydride repeat units stiffen the SMA backbone while TMPC repeat units, with their bulky methyl side groups, reduce the mobility of copolycarbonates. If solvent effects are exacerbated by limited molecular mobility, it is possible that the miscibility map may actually open to higher MA contents at low PC content in the copolycarbonate where mobility is the most restricted.

To identify and eliminate DCM solvent effects, blends

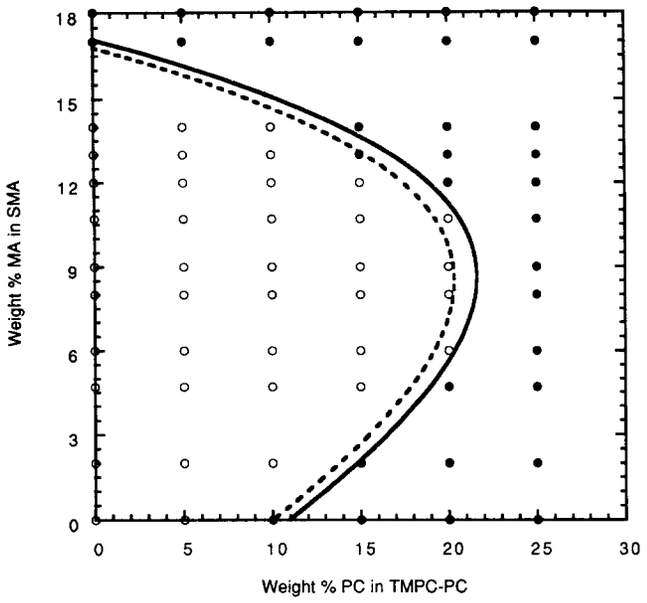

Figure 4 Isothermal miscibility map for 50/50 blends of SMA copolymers with TMPC–PC copolymers at 180°C. Empty circles, blends determined to be miscible by d.s.c.; filled circles, immiscible blends. The solid line was calculated using $B_{crit} = 0.032$ cal cm^{-3} and the set of best-fit interaction energies (cal cm^{-3}) determined to be $B_{TMPC/PC} = -0.1$, $B_{TMPC/PS} = -0.02$, $B_{TMPC/MA} = 9.6$, $B_{PC/PS} = 0.37$, $B_{PC/MA} = 8.3$, and $B_{PS/MA} = 10.6$. The broken line was calculated using the same set of interaction energies but with $B_{crit} = 0.028$ cal cm^{-3}

were hot-cast from THF and annealed at 180°C for 48, 96 and 144 h. An increased annealing time did not affect the observed phase behaviour; hence, 96 h of annealing was deemed adequate to ensure that equilibrium phase behaviour was observed. Furthermore, degradation was not evident in the glass transition behaviour, n.m.r. spectra, or in the molecular weights of sampled blends following this thermal treatment. *Figure 4* shows the complete isothermal miscibility map for the system of SMA and TMPC–PC blends prepared by THF hot casting. Compared to the map found for DCM-cast blends, the upper miscibility boundary is shifted to higher MA compositions. These results support the hypothesis that for this blend system, DCM casting can trap blends of limited molecular mobility in a two-phase, non-equilibrium state.

FLORY–HUGGINS ANALYSIS OF ISOTHERMAL MISCIBILITY MAP

The isothermal miscibility map defines the locus of blend compositions where the entropic contribution to mixing, calculated in terms of B_{crit} using equation (3), exactly balances the net B interaction, calculated using the appropriate form of the binary interaction model. Graphically fitting the theory to the experimental miscibility map in *Figure 4* requires that a single B_{crit} value be used to represent all blend compositions. However, use of a constant B_{crit} is appropriate only when there is only a small variation in molecular weights within each copolymer set and the quality of the fit is relatively insensitive to changes in B_{crit}. *Figure 5* shows the B_{crit} values calculated for each blend composition using equation (3) and information in *Table 1* and *2*. The shaded boxes correspond to the blends that lie along the miscibility boundary. An average B_{crit} value of 0.032 cal cm^{-3} accurately represents blends along the phase boundary with 4.7 wt.% or more MA in the SMA, while a smaller B_{crit} value of 0.028 better represents blends containing 2 wt.% and less MA. For B_{ij} evaluations, B_{crit} will be set at 0.032, keeping in mind that the actual fit at lower SMA compositions will be less favourable when the smaller B_{crit} is taken into account. Blends with TMPC83 were omitted from this analysis because a lower than average molecular weight makes its isothermal window of miscibility with SMA significantly wider than for neighbouring blends.

Using equation (4), $B_{crit} = 0.032$, and $B_{PS/MA}$ set at 10.6 cal cm^{-3}, the remaining interaction parameters were obtained by optimizing the fit of the phase boundary predicted by the binary interaction model to the experimental data. This process was aided by a computer program that minimizes the sum of the squares of the orthogonal distance between experimental data points and the predicted phase boundary[31]. The solid line shown in *Figure 4* represents the best fit of the isothermal miscibility map and was calculated from the Flory–Huggins theory with $B_{crit} = 0.032$ and the B_{ij} interaction energies listed in *Table 5*. The broken curve in *Figure 4* was calculated using the same set of B_{ij} interactions but with $B_{crit} = 0.028$. This change shifts the miscibility envelope to the left, owing to a reduction in the entropic contribution to mixing, and allows for an improved representation of the phase behaviour for blends with SMA compositions of 2 wt.% MA or less. Moreover, the quality of the predicted phase boundary does not lessen when the entropic contribution to miscibility is considered for each blend rather than an overall averaged B_{crit}. This was verified by calculating the net B interaction energy for each blend composition and comparing the value with the corresponding B_{crit}. The accurate prediction of miscibility or immiscibility was found in nearly every case. When the molecular weights of the omitted TMPC83 blends are taken into account, the model predicts the wider limits of miscibility that necessitated their exclusion from this analysis.

The isothermal phase boundary drawn in *Figure 4* is based on the set of best-fit B_{ij} interactions, but it should be recognized that a reasonable representation of the data can

Weight % MA in SMA	0	5	10	15	20	25
17	0.032	0.036	0.038	0.038	0.037	0.035
14	0.028	0.031	0.033	0.033	0.032	0.030
13	0.027	0.030	0.032	0.032	0.031	0.029
12.2	0.027	0.030	0.032	0.032	0.031	0.029
10.7	0.026	0.029	0.031	0.031	0.030	0.029
9	0.025	0.028	0.030	0.030	0.029	0.027
8	0.026	0.029	0.032	0.032	0.031	0.029
6	0.024	0.027	0.029	0.029	0.028	0.026
4.7	0.027	0.030	0.032	0.033	0.032	0.030
2	0.023	0.026	0.028	0.028	0.027	0.025
0	0.023	0.026	0.028	0.028	0.027	0.025

Weight % PC in TMPC/PC

Figure 5 B_{crit} values (cal cm^{-3}) as a function of blend composition. Shaded values correspond to blend compositions that lie along the isothermal phase boundary; $B_{crit} = 0.032$ represents an average value for blends along the phase boundary with 4.7 wt.% or more MA in the SMA. A smaller B_{crit} of 0.028 better represents blends with SMA containing 2 wt.% and less MA

Table 5 Binary interaction energies determined in this study at 180°C

Interaction pair	ΔP_{ij}^{*} (cal cm^{-3})	B_{ij} (cal cm^{-3})	Confidence limits for B_{ij} (cal cm^{-3})
TMPC/PC	−0.25	−0.1	± 0.1
TMPC/PC	−0.09 to −0.17	−0.02	± 0.01
TMPC/MA	9.9 to 10.4	9.6	± 0.2
PC/PS	0.40 to 0.41	0.37	± 0.05
PC/MA	8.8 to 9.1	8.3	± 0.5
PS/MA	11.3 to 11.6	10.6	± 0.2

still be realized with slight variations to this set. Confidence ranges for each B_{ij} value were evaluated by individually varying each parameter and determining whether a good fit to the data could be achieved by adjusting the remaining parameters; the last column in *Table 5* shows the limits estimated in this way. Thus, for any B_{ij} value that lies within its defined range of confidence, a set of interactions that accurately predict the isothermal phase boundary can be formulated using parameters from the confidence intervals prescribed for the remaining interactions. These ranges do not correspond to any quantifiable statistical significance but are provided to help give a feel for the confidence with which each parameter is known.

The Flory–Huggins interaction energies determined in this work are in excellent agreement with those from previous studies when temperature corrections are made, as seen by comparing B_{ij} values in *Table 3* and *5*, respectively. These results support the assumption that to a good approximation, the bare interaction energies from the Sanchez–Lacombe theory are independent of temperature, and that the temperature dependence of Flory–Huggins-type interactions arises from equation-of-state effects. Furthermore, it demonstrates the effectiveness of the accounting procedures of the binary interaction model. In addition to the verification and refinement of previously determined interaction energies, interaction energies for TMPC/MA and PC/MA were found to be $B_{\mathrm{TMPC/MA}} = 9.6$ cal cm^{-3} and $B_{\mathrm{PC/MA}} = 8.3$ cal cm^{-3}.

PREDICTED PC/SMA INTERACTION ENERGY

The interaction of PC with SMA as a function of the maleic anhydride content in the latter can be calculated using the interaction energies for PC/PS, PC/MA and PS/MA given in *Table 5* and the following form of the binary interaction model

$$B_{\mathrm{PC/SMA}} = B_{\mathrm{PC/PS}}\phi_{\mathrm{S}}' + B_{\mathrm{PC/MA}}\phi_{\mathrm{MA}}' - B_{\mathrm{PS/MA}}\phi_{\mathrm{S}}'\phi_{\mathrm{MA}}' \tag{13}$$

A plot of $B_{\mathrm{PC/SMA}}$ *versus* SMA composition is shown in *Figure 6*, and includes, for comparison, the interaction between PC and SAN. The latter curve is based on refined PC/AN and PS/AN interactions determined by Callaghan *et al.*[1] appropriately adjusted to 180°C using AN characteristic parameters reported elsewhere[31]. Both curves show a minimum at a certain copolymer composition; this occurs at about 16 wt.% MA for SMA and about 21 wt.% AN for SAN. The minimum PC interaction energy with SAN is more favourable than the minimum PC interaction with SMA. When these curves were recalculated at 270°C to investigate how interactions might change under processing conditions, the PC/SMA curve was altered negligibly while the minimum in the PC/SAN interaction shifted upward by around 0.02 cal cm^{-3}, nearly one-third of the difference between the two minimum values at 180°C.

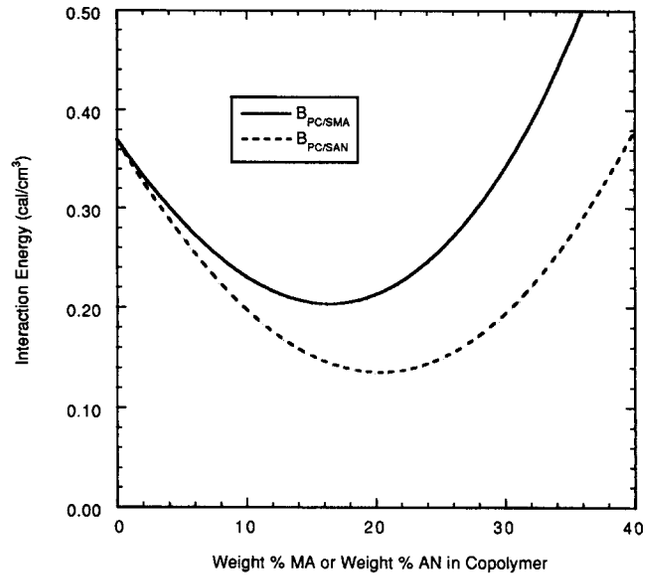

Figure 6 Calculated Flory–Huggins interaction energies at 180°C for polycarbonate with SMA (solid line) and SAN (broken line) as a function of copolymer composition. Curves are based on the following binary interaction parameters (cal cm^{-3}) $B_{\mathrm{PC/PS}} = 0.37$, $B_{\mathrm{PC/MA}} = 8.3$, $B_{\mathrm{PC/AN}} = 4.8$, $B_{\mathrm{PS/MA}} = 10.6$ and $B_{\mathrm{PS/AN}} = 7.0$

PHASE SEPARATION BEHAVIOUR

The temperatures at which phase separation occurs on heating were determined for blends found miscible at 180°C and are reported inside the circles at each blend composition in *Figure 7*. The notation < 180 indicates blends that were assessed to be immiscible at 180°C while > 300 indicates that phase separation on heating was not observed prior to thermal degradation. A reversal of phase separation behaviour was confirmed for blends at several locations within the miscibility envelope, but often required several hours of annealing and special precautions to avoid thermal degradation. For many blends, the phase separation process could not be reversed because the phase separation temperature was too close to the blend T_{g}. In these cases, the polymer chains lack the mobility and the thermodynamic driving force necessary to allow homogenization of the two-phase mixture by diffusion within a reasonable amount of time. At higher temperatures, degradation proved to be a particular concern. For example, when a miscible blend of TMPC95 with SMA14 was annealed at 275°C, phase separation was observed within 5 min by the development of two T_{g}s, but additional annealing for 10 min led to a single T_{g} again. An n.m.r. analysis helped to identify degradation as the cause of this unusual phase behaviour.

EQUATION-OF-STATE ANALYSIS OF PHASE BEHAVIOUR

It is possible, in principle, to obtain an independent evaluation of interaction energies using phase separation temperatures evaluated at several blend compositions[4]. This requires calculation of ΔP^{*} for each blend using the equation-of-state theory followed by a regression of these values *versus* copolymer composition to the binary interaction model, equation (9). However, for such an analysis to be statistically significant, more data points must be known than are available for this blend system. Alternatively, the above equation-of-state analysis can be used

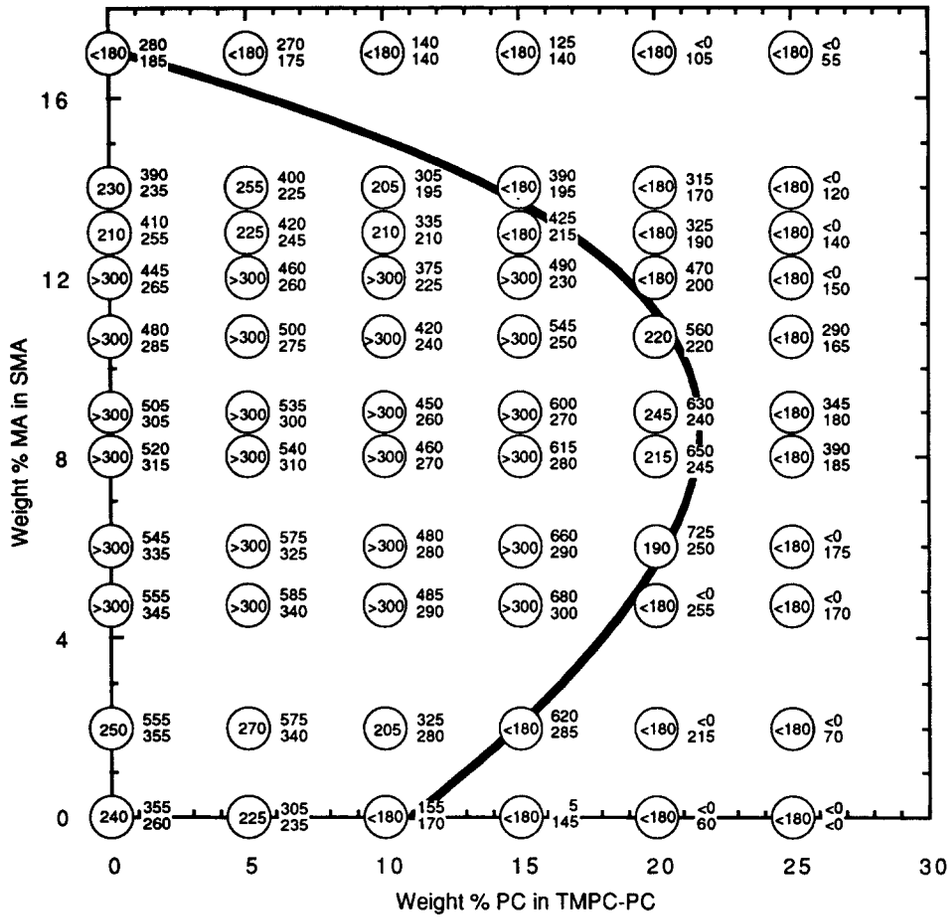

Figure 7 Isothermal miscibility map showing experimentally measured phase separation temperatures (°C) of the LCST-type given inside the circle at each blend composition. A value greater than 180 indicates that the blend was deemed miscible at the isothermal condition of 180°C, the notation < 180 indicates that the blend was found to be immiscible at 180°C, and the notation > 300 indicates that phase separation could not be observed prior to thermal degradation of the sample. Phase separation temperatures predicted by the equation-of-state theory are given to the immediate right of the circles containing the experimental values; the two values shown were calculated using characteristic parameters for PS and SMA noted in *Table 4* for the 180–230°C and 220–270°C temperature ranges, corresponding to the upper and lower numbers, respectively

in reverse to predict phase separation temperatures when interaction energies are known. Predicted values may then be compared to experimental phase separation temperatures.

For this study, the B_{ij} values determined in the isothermal analysis were converted to ΔP^*_{ij} using equation (10), and spinodal temperatures were estimated using equation (8). Both calculations make use of the appropriate characteristic parameters provided in *Table 4*. The ranges reported for several of the converted ΔP^*_{ij} values shown in *Table 5* demonstrate the effect of using the various temperature-dependent characteristic parameter sets. *Figure 7* includes two predicted phase separation temperatures shown to the immediate right of each measured temperature. The top value was predicted using a set of characteristic parameters from *Table 4* that include PS and MA parameters for the 180–230°C temperature range, while the bottom value was calculated using PS and MA parameters for the 220–270°C range. The large difference in the predicted temperature reveals that predictions by the equation-of-state theory are quite sensitive to the characteristic parameters used in the calculations. Considerably improved predictions are obtained when the parameter sets for the 220–270°C range are used *versus* those for the 180–230°C range, owing to maximum differences in P^*, T^* and ρ^* of approximately 35%, 10% and 2%, respectively. The greatest of these differences are in the MA characteristic parameters and are a consequence of the extrapolation of SMA copolymer parameters to a homopolymer of MA. The differences between the various parameter sets also stem from errors in *PVT* data, and to a greater extent, from the fact that the equation of state does not perfectly describe the form of the *PVT* data[49]. In this light, it is remarkable that the second set of predicted phase separation temperatures demonstrates such a reasonable correspondence with the isothermal phase boundary evaluated at 180°C and with individual phase separation temperatures, including their trends with changing copolymer composition. Although blends with TMPC83 were left out of this analysis for the purpose of presentation, the phase separation temperatures predicted for these blends agree well with experimental observations.

All phase observations made in this study have been assumed to represent the spinodal condition for the purpose of simplified calculations. Spinodal- and binodal-type phase boundaries overlap at the critical blend composition which, for blends of polymers having similar molecular weights, is at or near a 50/50 blend ratio. To help ensure evaluation of the spinodal, blends up to this point in the study were prepared with 50/50 ratios. However, the critical composition can drift toward the lower molecular weight component as the difference in the molecular weights increases. As the critical blend composition shifts further from the centre of the phase diagram, it becomes more likely that phase behaviour observations do not correspond to the spinodal.

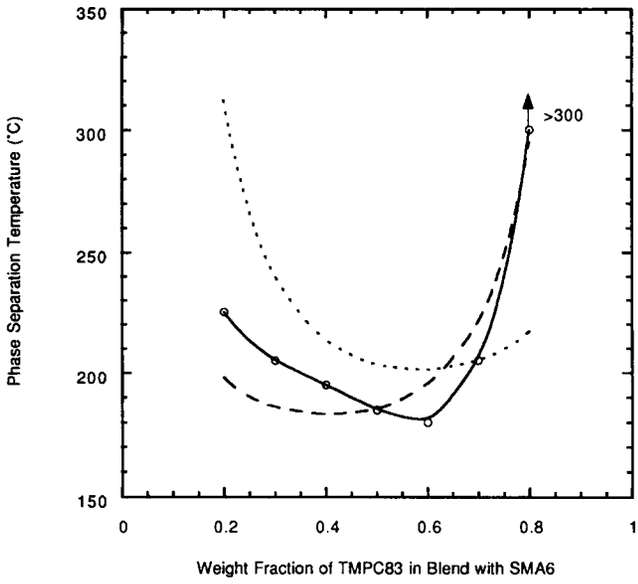

Figure 8 Phase separation temperatures for blends of SMA6 with TMPC83 as a function of blend composition. Experimentally determined phase separation temperatures (O) are compared with the spinodal curve predicted from the equation-of-state theory using ΔP^* for a 50/50 critical blend composition (dashed line) and using ΔP^* for a 70/30 critical blend composition (dotted line)

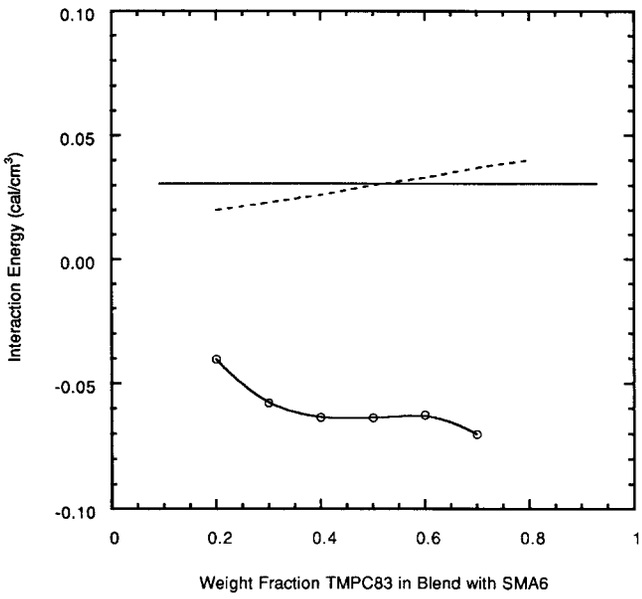

Figure 9 Composition dependence of the bare interaction parameter ΔP^* (O) calculated from the experimental phase separation temperatures shown in *Figure 8* and using SMA6 characteristic parameters for the 220–270°C temperature range. B_{sc} is calculated as a function of composition using equation (10) and ΔP^* for a 50/50 blend (broken line), and compared to the composition invariant B_{sc} calculated using the results from the isothermal analysis (solid line)

To investigate the magnitude of this effect and the accuracy of the spinodal assumption, blends of TMPC83 and SMA6 of different compositions were prepared by hot casting from THF. All the blends were found to have single glass transition temperatures with values that track continuously with blend ratio between the T_gs of the neat copolymers. *Figure 8* shows the phase separation temperatures evaluated for each blend composition. A ΔP^* value was calculated from each phase separation temperature using equation (8) and the appropriate characteristic parameters from *Table 4*, and then plotted *versus* blend composition in *Figure 9*. The values of ΔP^* are small and negative and have a weak composition dependence. This dependence may have been caused by the calculation of ΔP^* values from phase separation temperatures that do not correspond to the spinodal curve — a problem that, as discussed above, can occur at blend ratios removed from the critical composition.

If ΔP^* is assumed to be a constant, equation (8) can be used to predict a spinodal phase boundary. Such calculations using ΔP^* evaluated for a 50/50 blend and using ΔP^* for a 70 wt.% TMPC83 blend are shown in *Figure 8* along with experimental phase separation temperatures. The 70/30 blend is the theoretically predicted critical composition. Both of the predicted spinodal diagrams reflect the general shape of the experimental phase boundary and the relative magnitude of the phase separation values, but the 50/50 based calculation seems to be a better representation of the experimental data, especially at the higher TMPC83 compositions. Nonetheless, the small difference between the experimental phase separation temperatures for a 50/50 *versus* a 70/30 blend suggests that the potential error associated with the use of slightly off-critical blend compositions is not a serious liability to the accuracy of the interaction energies determined in this study.

Furthermore, using the ΔP^* evaluated for a 50/50 blend, the net Flory–Huggins interaction energy density at the spinodal condition, B_{sc}, can be calculated using equation (10). *Figure 9* compares these calculations to a composition invariant B_{sc} estimated using the interaction energies from the isothermal study. Nearly perfect agreement for 50/50 blends is shown and the deviations for other blend compositions are minor. The small positive B_{sc} predicted by either method is offset by entropic contributions, as miscibility is observed for these blends at 180°C.

CONCLUSIONS

Selective phase diagram information and an isothermal miscibility map for blends of SMA copolymers with TMPC–PC copolycarbonates were determined. A window of miscibility exists in the isothermal miscibility map of SMA copolymer *versus* copolycarbonate composition where the SMA contains less than 17 wt.% MA and the copolycarbonate contains less than 25 wt.% PC. The S/MA interaction energy was independently evaluated using a copolymer-modified critical molecular weight analysis, and the remaining interactions were evaluated from the above-mentioned miscibility map using the Flory–Huggins theory and the binary interaction model. All values are in excellent agreement with previously estimated interactions after equation-of-state temperature corrections were performed using the Sanchez–Lacombe lattice fluid theory. In addition, TMPC/MA and PC/MA binary interactions were quantified and found to be large positive values; both are less favourable than those reported elsewhere for the TMPC/AN and PC/AN interactions. Using the binary interaction energies evaluated in this study, the PC/SMA interaction energy was calculated and a minimum was found to occur at around 16 wt.% MA. This minimum is not as favourable as that reported for blends of PC with SAN copolymers. An equation-of-state prediction of phase separation temperatures was found to be very sensitive to the equation-of-state characteristic parameters. Nonetheless, within the ranges of the parameter sets investigated, the analysis was able to predict phase separation

temperatures that show reasonable agreement with experimental observations.

ACKNOWLEDGEMENTS

The assistance of Sanjay Gupta in the preparation and evaluation of blends for the critical molecular weight analysis is kindly acknowledged. Financial support for this work has been provided by the National Science Foundation grant number DMR 92-15926 administered by the Division of Material Research — Polymers Program.

REFERENCES

1. Callaghan, T. A., Takakuwa, K. and Paul, D. R., *Polymer*, 1993, **34**, 3796.
2. Guest, M. J. and Daly, J. H., *Eur. Polym. J.*, 1990, **26**, 603.
3. Keitz, J. D., Barlow, J. W. and Paul, D. R., *J. Appl. Polym. Sci.*, 1984, **29**, 3131.
4. Kim, C. K. and Paul, D. R., *Polymer*, 1992, **33**, 4941.
5. Kurauchi, T. and Ohta, T. J., *J. Mater. Sci.*, 1984, **19**, 1699.
6. Kwei, T. K., Frisch, H. L., Radigan, W. and Vogel, S., *Macromolecules*, 1977, **10**, 157.
7. McLaughlin, K. W., *Polym. Eng. Sci.*, 1989, **29**, 1560.
8. Mendelson, R. A., *J. Polym. Sci., Polym. Phys. Ed.*, 1975, **1985**, 23.
9. Nishi, T., Suzuki, T., Matsuzawa, N., Michizono, S. and Tanaka, H., *Polym. Prepr.*, 1987, **28**, 110.
10. Paul, D. R., *Macromol. Symp.*, 1994, **78**, 83.
11. Quintens, D., Groeninckz, G., Guest, M. and Aerts, L., *Polym. Eng. Sci.*, 1991, **31**, 1207.
12. Stretz, H. A., Cassidy, P. E. and Paul, D. R., *Polym. Mater. Sci. Eng.*, 1997, **76**, 493.
13. Gan, P. P. and Paul, D. R., *J. Appl. Polym. Sci.*, 1994, **54**, 317.
14. Paul, D. R. and Barlow, J. W., *Polymer*, 1984, **25**, 487.
15. Kambour, R. P., Bendler, J. T. and Bopp, R. C., *Macromolecules*, 1983, **16**, 753.
16. ten Brinke, G. and Karasz, F. E., *Macromolecules*, 1984, **17**, 815.
17. Flory, P. J., *J. Chem. Phys.*, 1942, **10**, 51.
18. Huggins, M. L., *J. Chem. Phys.*, 1941, **9**, 440.
19. Koningsveld, R. and Chermin, H. A. G., *Proc. R. Soc. London, Ser. A*, 1970, **319**, 331.
20. Koningsveld, R. and Schoffeleers, H. M., *Pure Appl. Chem.*, 1974, **39**, 1.
21. Koningsveld, R., *Br. Polym. J.*, 1975, **7**, 435.
22. Koningsveld, R. and Kleintjens, L. A., *J. Polym. Sci., Polym. Symp.*, 1977, **61**, 221.
23. Sanchez, I. C. and Lacombe, R. H., *J. Phys. Chem.*, 1976, **80**, 2352.
24. Sanchez, I. C. and Lacombe, R. H., *J. Polym. Sci., Polym. Lett.*, 1977, **15**, 71.
25. Sanchez, I. C. and Lacombe, R. H., *Macromolecules*, 1978, **11**, 1145.
26. Sanchez, I. C., *Annu. Rev. Mater. Sci.*, 1983, **13**, 387.
27. Sanchez, I. C., in *Encyclopedia of Physical Science and Technology*, Vol. 11, ed. R. A. Meyers, Academic Press, New York, 1987.
28. Sanchez, I. C., *Polymer*, 1989, **30**, 471.
29. Sanchez, I. C., *Macromolecules*, 1991, **24**, 908.
30. Callaghan, T. A., Ph.D. Dissertation, The University of Texas at Austin, 1992.
31. Gan, P. P., Ph.D. Dissertation, The University of Texas at Austin, 1994.
32. Kim, C. K. and Paul, D. R., *Polymer*, 1992, **33**, 1630.
33. Gupta, S., Masters Dissertation, The University of Texas at Austin, 1995.
34. Bohn, L., in *Polymer Handbook*, ed. J. Brandrup and E. H. Immergut, Wiley–Interscience, New York, 1975, pp. 111-211.
35. Callaghan, T. A. and Paul, D. R., *J. Polym. Sci.: Part B: Polym. Phys.*, 1994, **32**, 1813.
36. Guo, W. and Higgins, J. S., *Polymer*, 1990, **31**, 699.
37. Brereton, M. G., Fisher, E. W. and Herkt-Maetzky, C., *J. Chem. Phys.*, 1987, **10**, 6144.
38. Yang, H. and O'Reilly, J. M., *Mater. Res. Soc. Symp. Proc.*, 1987, **79**, 129.
39. Kim, C. K. and Paul, D. R., *Polymer*, 1992, **33**, 4929.
40. Kambour, R. P., Gundlach, P. E., Wang, I. C. W., White, D. M. and Yeager, G. N., *Polym. Commun.*, 1988, **29**, 170.
41. Callaghan, T. A. and Paul, D. R., *Macromolecules*, 1993, **26**, 2439.
42. Fox, T. G., *Bull. Am. Phys. Soc.*, 1956, **1**, 123.
43. Robard, A., Patterson, D. and Delmas, G., *Macromolecules*, 1977, **10**, 706.
44. Zeman, L. and Patterson, D., *Macromolecules*, 1972, **5**, 513.
45. Nandi, A. K., Mandal, B. M. and Bhattacharyya, S. N., *Macromolecules*, 1985, **18**, 1454.
46. Woo, E. M., Barlow, J. W. and Paul, D. R., *J. Polym. Sci., Polym. Symp.*, 1984, **71**, 137.
47. Chiou, J. S., Barlow, J. W. and Paul, D. R., *J. Polym. Sci.: Part B: Polym. Phys.*, 1987, **25**, 1495.
48. Nishimoto, M., Keskkula, H. and Paul, D. R., *Polymer*, 1991, **32**, 272.
49. Rodgers, P. A., *J. Appl. Polym. Sci.*, 1993, **48**, 1061.